

A Model of Baryons

R Wayte

29 Audley Way, Ascot, Berkshire SL5 8EE, England, UK.

email: rwayte@googlemail.com

Research article. Submitted to vixra.org 10 October 2011

Abstract.

Baryons are considered to be intricate particles having real geometrical structure, based on our previous proton design. Inherent baryon spin is proportional to mass and radius. The well-known octets and decuplets fit into groups where mass-squared and quantised-action are related. Magnetic moments are described in terms of a positive spin-loop and orbiting temporary electron(s). Lifetime of a baryon is governed by action of guidewave coherence around these structures.

Key words: baryon composite models

PACS Codes: 12.60.Rc, 14.20.Gk, 14.20.Jn, 13.30.Eg

1. Introduction

Baryons are considered here to be complicated particles related to the previous proton and meson designs (Wayte, Papers 1, 2). Three trineons, bound together by their gluon field, travel at the velocity of light around the spin-loop. There may also be a core particle at the centre of the spin-loop which has zero net angular momentum. The remaining mass energy consists of an external non-rotating pionic-type field, emitted by the trineons and core, plus a small amount of electromagnetic field energy. Little mention of QCD theory has been necessary to develop this model, wherein quarks possess spin yet are theoretical points of zero size and infinite density; see Amsler et al (2008). In practice, the QCD model is an "equivalent black-box" solution crafted to describe how particles behave towards each other, but it is not an accurate representation of the internal reality. Appendix A shows how the conceptual differences between these models can be explained, if particles in collisions can generate aspects not immediately apparent in static models. This makes the QCD model correct in essence for describing interactions, but inadequate in its application to the real mechanisms of particles. Mass is entirely due to localised circulating energy, so the Higgs mechanism is unnecessary.

In Section 2, the increase in particle angular momentum with mass-squared, for some baryons, is investigated to reveal an underlying action principle. The well known octets and decuplets are grouped here but other groups appear discordant. Section 3 covers strangeness. Sections 4 and 5 explain magnetic moments and lifetimes in a way analogous to the proton and neutron, that is, the positive baryon spin-loop may be orbited by one or two temporary heavy-electrons.

2. Spin relative to mass-squared for some baryons

From the complete range of baryons, some were found to indicate a tendency for J to increase with mass-squared M^2 , as demonstrated in a Chew-Frautschi plot. This does not look random and is thought to result from a particular mechanism in those baryons. Figure 2.1 illustrates cases in which two or more particles of a given species lie on a straight line trajectory parallel to the Δ and Λ standards, but some of these may still be coincidences. The parallel lines are found to obey the expression:

$$M^2 \approx 2(J + A)\delta^{-4}m_e^2 \quad , \quad (2.1)$$

where ($\delta = 1/12\pi \approx 1/37.7$) is the proton pearl structure constant from Paper 1, m_e is the electron mass, and A represents extra mass which increases M beyond that which contributes to the spin. Although A varies considerably, it appears to be a multiple of (1/6), so it may be combined with J to get $[(J+A) = N/6]$ for integral N. Equation (2.1) then becomes:

$$M^2 \approx (N/3)(37.7^2 m_e)^2 \quad ; \quad (2.2a)$$

and this expression can take other forms for later analysis:

$$M^2 \approx 3N \times [3 \times 137(\pi/e_n)]^2 m_e^2 \approx N(6 \times 137)^2 m_e^2, \quad (2.2b)$$

where 137 is the inverse fine structure constant and (π/e_n) has previously signified gluon involvement. Factor 3 may derive from the 3 trineons with their associated gluons and mesons.

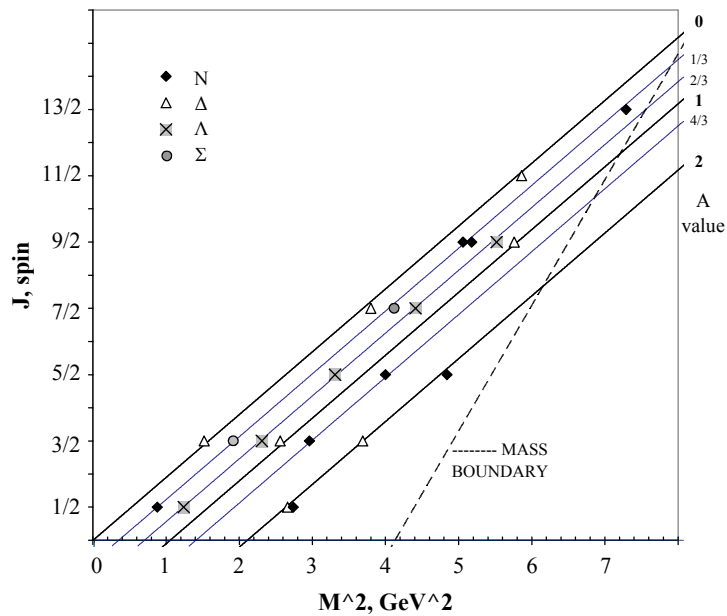


Figure 2.1 Selected baryons which lie on straight parallel lines, obeying Eq.(2.1) for various values of A given.

To interpret these expressions in terms of baryon structure, we will assume that J represents real angular momentum of a spin-loop due to mass M_1 as in the proton, but A represents an object of mass M_2 with zero net spin at the very centre. Many mesons analysed in Paper 2 have this design; consequently, we can write an *action* expression:

$$\left(\frac{M_1}{2}\right)cR2\pi + \left(\frac{M_2}{2}\right)c^2\tau = (J + A)h \quad , \quad (2.3a)$$

where spin radius is proportional to mass ($R = F_b M/c^2$), and the spin period is ($\tau = 2\pi R/c$). Then the first term is spin-action over one orbit, and the second term is the concomitant static-action of the core mass. As found for the proton, only half the mass ($M_1/2, M_2/2$) is involved in this expression because half is in the exterior field. Now, ($M = M_1 + M_2$), therefore:

$$(J + A)h = \frac{M}{2}cR2\pi = 2\pi\left(\frac{F_b}{c}\right)\frac{M^2}{2} \quad , \quad (2.3b)$$

and using Eq.(2.1), the constant F_b is:

$$F_b \approx \frac{137}{37.7^4} \left(\frac{e^2}{m_e^2}\right) \quad . \quad (2.4)$$

The spin-mass and core-mass are given by:

$$M_1 = M\left(\frac{J}{J + A}\right); \quad M_2 = M\left(\frac{A}{J + A}\right); \quad \frac{M_2}{M_1} = \frac{A}{J} \quad , \quad (2.5)$$

and these do not appear to take any special noteworthy values for the Λ 's and Δ 's in Figure 2.1. Coefficient N does not *in general* represent the number of component pieces constituting M , but this might apply to some baryons, see Table 1a. The Δ 's with ($A = 0$) have no core particles. In high energy p-p collisions, J and A appear somewhat arbitrary in created particles but take quantised values satisfying M_1 and M_2 in Eq.(2.5).

Equations (2.3a,b) confirm the fermion spin radius R for the spinning mass M_1 , and R is also defined by total mass M :

$$R = \frac{2J\hbar}{M_1 c} = \frac{2(J + A)\hbar}{M c} = \frac{F_b M}{c^2} \quad . \quad (2.6a)$$

For stability there is an integral number of Compton guidewavelengths around the spin-loop:

$$2\pi R = 2J(h/M_1 c) \quad . \quad (2.6b)$$

Plots of A versus J are shown in Figure 2.2 for five baryon species. Within the diagonal boundary lines, it appears that A accommodates the prevailing J almost arbitrarily, probably because many particles are not designed to obey Eq.(2.1). In the case of Λ and Ξ particles there could be a zone of avoidance for small A . The total

plot shows how certain A values are common while others are vacant; and some intervals *between* particles are preferred. Therefore, some values of N must be preferred, which will affect M^2 and particle action. However, the overall lack of order implies that a further mass law operates for the particles not simply covered by Eq.(2.1).

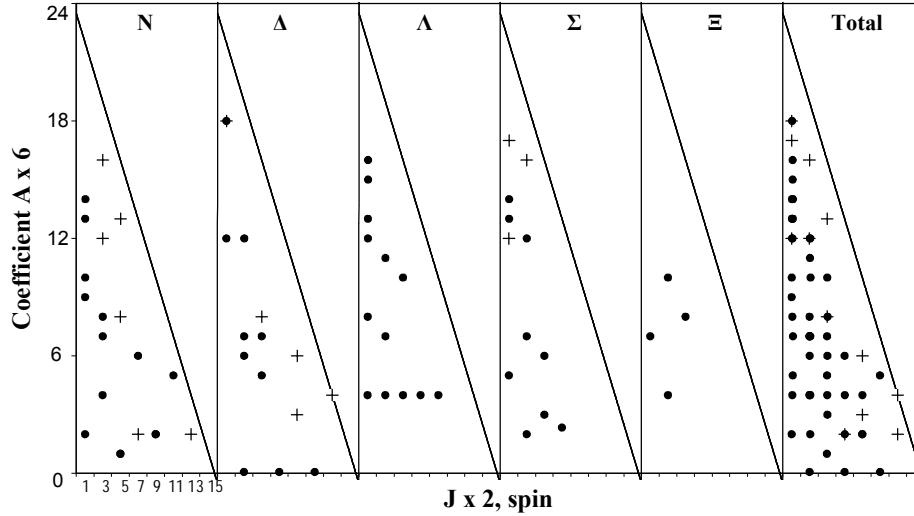


Figure 2.2 Plots to show how factor A varies with spin J for each type of baryon. The points lie within a common boundary line, but Λ s and Ξ s may have a zone of avoidance at low A values. Baryons of 2-star quality have also been included (+).

The diagonal boundary line in Figure 2.2 describes A through the form:

$$A_b = -\frac{3}{6}J + \frac{23.5}{6} \quad (2.7a)$$

It cuts the abscissa at ($2J_{\max} = 15.667$, $A = 0$) where the maximum possible baryon mass takes a specific value through Eq.(2.1):

$$M_{\max} = 2875\text{MeV} \quad (2.7b)$$

This mass is just beyond the point where 3 trineons can become 3 protons. At the other end ($J = 0$, $A_{\max} \approx 23.5/6$), the baryon mass is only:

$$M = M_{\max} / \sqrt{2} \quad (2.7c)$$

so A is more limited than J, ($A_{\max} = J_{\max}/2$). Upon introducing Eq.(2.7a) into Eq.(2.1), a corresponding mass boundary may be drawn on Figure 2.1 as shown, for:

$$M_b^2 \approx 2 \times \left[\left(\frac{3}{6}J + \left(\frac{23.5}{6} \right) \right) (37.7^2 m_e)^2 \right] \quad (2.8)$$

Some quantisation of baryon mass-squared given by N in Eq.(2.2a) may also be plotted to reveal *patterns*, as in Figure 2.3a. *All* confirmed baryons are included but those linked by an increment ($\Delta N = 6, 12$) have been emphasised as the Os and Xs. Figure 2.3b illustrates groups of particles with the same spin-parity, including the well-known baryon octet $(\frac{1}{2})^+$, decuplet $(\frac{3}{2})^+$, groups $(\frac{5}{2})^+$ and $(\frac{7}{2})^+$. These do not show special regard for the distribution in Figure 2.3a, thereby confirming that A is not predictably connected to J .

The most common value of N in Figure 2.3a is 16, where for example ($J = 3/2^+ \bar{}$), and ($A = 7/6$) if Eq.(2.1) is applicable. Alternatively, Eq.(2.2a) evaluates to:

$$M \approx 1677 \text{MeV}/c^2 \approx 4\sqrt{N}m_x, \quad (2.9)$$

for ($m_x = 104.8 \text{MeV}/c^2$), which is between the muonic mass ($m_\mu = 105.66 \text{MeV}/c^2$) and the proton-pearl mass ($m_p/9 = 104.25 \text{MeV}/c^2$). However, this does not mean that there are 16 pearls in these particles because N concerns *action*, see Eq.(2.10). For comparison, in our proton model there are 9 pearls, while N is 5.

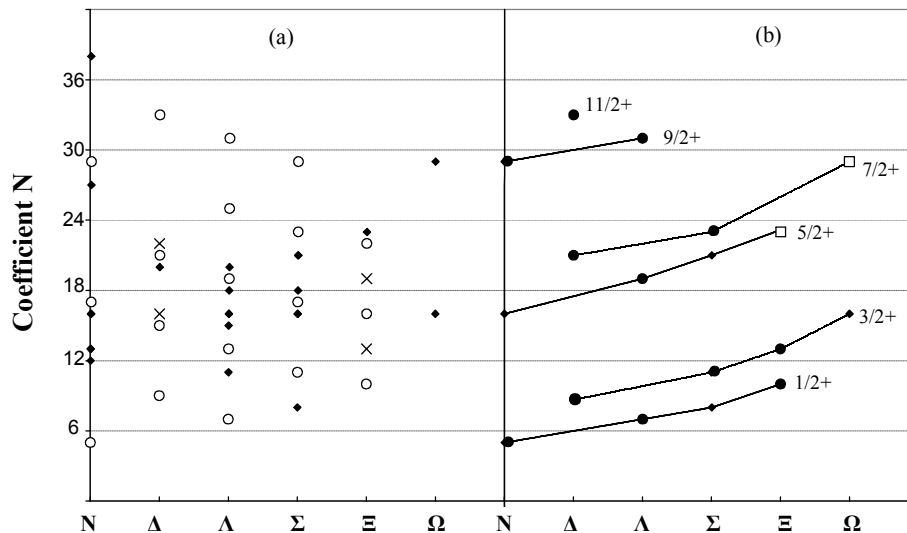


Figure 2.3 (a) Quantisation number N plotted for the six types of well observed baryons, to reveal patterns. The Os and Xs are the noteworthy points of a pattern linked by ($\Delta N = 6, 12$). (b) The grouping of particles with the same spin-parity into octet, decuplet and smaller groups reveals that there is limited correspondence between these and the distribution in part (a). Particles shown here and later as \square need confirmation.

Except for the Λ s and Δ s on the lines in Figure 2.1, it is impossible to know how N should be split into J and A components. For example, the proton has ($N = 5$) which could imply that ($A = 1/3$) for a particle core, but this would be wrong even though Eq.(2.2a) is numerically correct. Consequently for many particles, the N value may not be interpretable as $6(J + A)$, and for the proton it would be ($N = 10J$). For such particles with no central core, the material is all in the spin-loop at a radius which decreases inversely with mass but increases with J as in Eq.(2.6a) when ($M_1 \rightarrow M$), or can be expressed alternatively as in Eq.(2.10f).

In Figure 2.3a, the obvious pattern repetition for N incrementing by ($\Delta N = 6$) may be explained by introducing it into Eq.(2.3b) to produce a precise *action increment* for certain baryons:

$$\left[\frac{\Delta N}{6} \right] h = h \approx \Delta \left[\frac{M}{2} c 2\pi R \right] \approx \Delta \left[2\pi \frac{F_b}{c} \frac{M^2}{2} \right] ; \quad (2.10a)$$

or for the baryon mass-squared, Eq.(2.2a) gives:

$$\Delta(M^2)_6 \approx 2 \times (37.7^2 m_e)^2 . \quad (2.10b)$$

Therefore, these baryon sets increase mass-squared by *adding action quanta*, not by *multiplying* original masses by special factors. The way that the different species so clearly show this ($\Delta N = 6$) increment implies that they have similar mechanisms. Many smaller action increments occur because $\Delta N = 4, 3,$ or 2 are popular intervals.

When we set ($\Delta N = 1$) say, then Eq.(2.2a) can be reduced to:

$$\Delta(M^2)_1 \approx \left(\frac{37.7^2}{\sqrt{3}} m_e \right)^2 \approx (6 \times 137 m_e)^2 , \quad (2.10c)$$

which looks interesting because the nucleon-nucleon force constant is ($1/\sqrt{3}$) in Paper 1; therefore this expression contains 3 fundamental constants. For the popular absolute value ($N = 16$) this becomes:

$$(M^2)_{16} \approx (24 \times 137 m_e)^2 , \quad (2.10d)$$

which reflects the 24 gluonic loops per pearl seen in the proton.

There are several examples of N increasing by 6 in Figure 2.3a, beyond those satisfying Eq.(2.3b), so it is possible that *all* baryon masses are determined primarily by *action* related to M^2 . Equations (2.3b) and (2.4) would then define particle action in terms of N as:

$$Nh \approx M^2 \left(\frac{137}{2 \times 37.7^3} \right) \left(\frac{e^2}{m_e^2 c} \right) . \quad (2.10e)$$

And if all the mass is in the spin-loop, the spin radius must be reduced to:

$$R = \frac{2J\hbar}{Mc} = \left(\frac{6J}{N} \right) \left(\frac{F_b}{c^2} M \right) . \quad (2.10f)$$

A good example of this is $\Delta(1600)$, which would fit well on the ($A = 0$) line at ($J = 5/2$) in Figure 2.1, but chooses ($J = 3/2$) even though there is no core particle for Δ resonances. Other high mass baryons with small spin can be accommodated similarly.

In Figure 2.3b, octet $J^P = 1/2^+$, and groups $J^P = 5/2^+$ and $J^P = 9/2^+$, (N, Λ, Σ, Ξ) are related approximately through mass-squared following Eq.(2.1). Likewise, decuplet $J^P = 3/2^+$, and groups $J^P = 7/2^+$ and $J^P = 11/2^+$, ($\Delta, \Sigma, \Xi, \Omega$) are similarly related. The difference between these groups where ($\Delta N \approx 12$) in Eq.(2.2a) may be expressed as:

$$(M_5^2 - M_1^2) \approx (M_9^2 - M_5^2) \approx (M_7^2 - M_3^2) \approx [2(37.7)^2 m_e]^2 . \quad (2.11)$$

Since this is a square-law relationship, the actual mass of an M_5 baryon relative to its M_1 baryon depends upon the species: N, Λ, Σ, Ξ . Consequently, the M_5 baryons are simply heavier versions of the M_1 baryons, using the same design but specifically satisfying the expressions involving *action h* like Eq.(2.10a,b). The same applies to ($M_9 - M_5$) and ($M_7 - M_3$) groups. Given that ($\Delta J = 2$) here, then ($\Delta A \approx 0$), so individual A values in *these selected* baryons change very little as J increments. The ordinate positioning of the octet group and decuplet group implies that they have consistently different designs, such that the decuplet group is deficient in N by 3 due to low A values. If this deficiency were restored, then all the groups would be separated by ($\Delta N \approx 6$), as J increases.

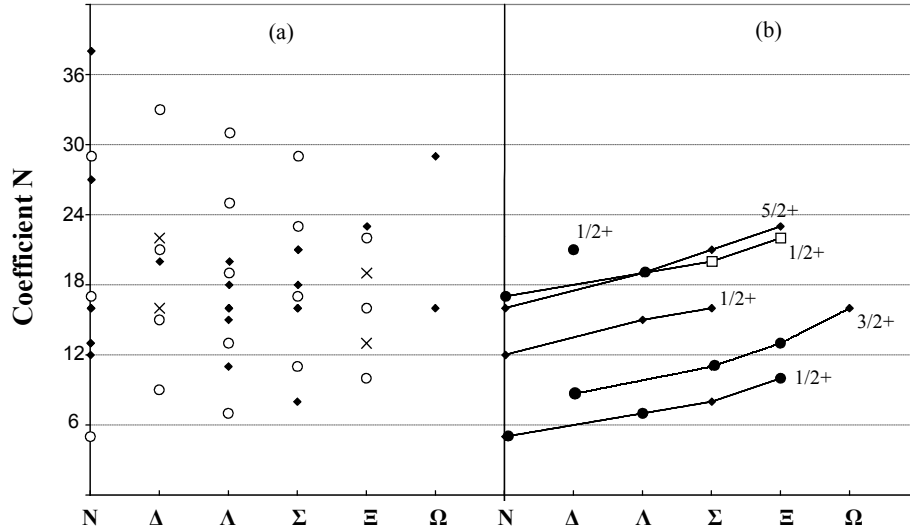


Figure 2.4 (a) Quantisation number N plotted for the six types of baryon.
 (b) The higher ($J^P = 1/2^+$) groups are shown relative to ($J^P = 5/2^+$), ($J^P = 3/2^+$) and ($J^P = 1/2^+$).

Figure 2.4b shows the second ($J^P = 1/2^+$) group as having N values greater than the lowest octet by ($\Delta N \approx 7-8$). The third ($J^P = 1/2^+$) group runs parallel to the lowest octet at ($\Delta N \approx 12$), so *action* equation (2.10a) is clearly operating. Baryons in these more massive groups are relatively compact, obeying Eq.(2.6) for a small A value.

Figure 2.5b also shows the lowest ($J^P = 1/2^-$) group as having excessive mass, with ($\Delta N \approx 8-9$) relative to the lower ($J^P = 1/2^+$) octet. Again, these baryons must be relatively small, to contain the extra mass without increasing spin.

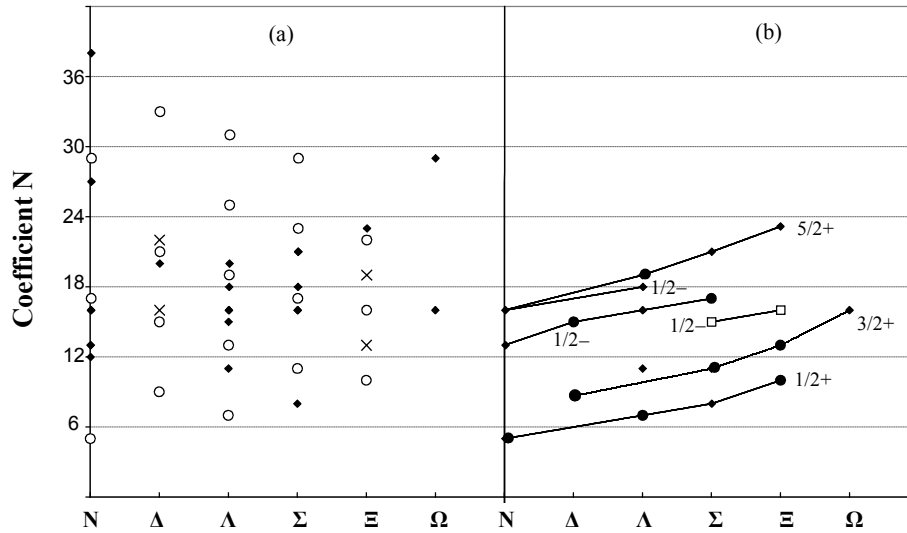


Figure 2.5 (a) Quantisation number N plotted for the six types of baryon.
 (b) The ($J^P = 1/2^-$) groups are shown relative to ($J^P = 5/2^+$), ($J^P = 3/2^+$) and ($J^P = 1/2^+$).

Figure 2.6b shows the ($J^P = 3/2^-$) group as having excessive N values; eg., ($\Delta N \approx 6$) relative to the lower original ($J^P = 3/2^+$) decuplet. The higher mass ($J^P = 3/2^-$) groups are also shown, at ($\Delta N \approx 9 - 12$) above the lower group.

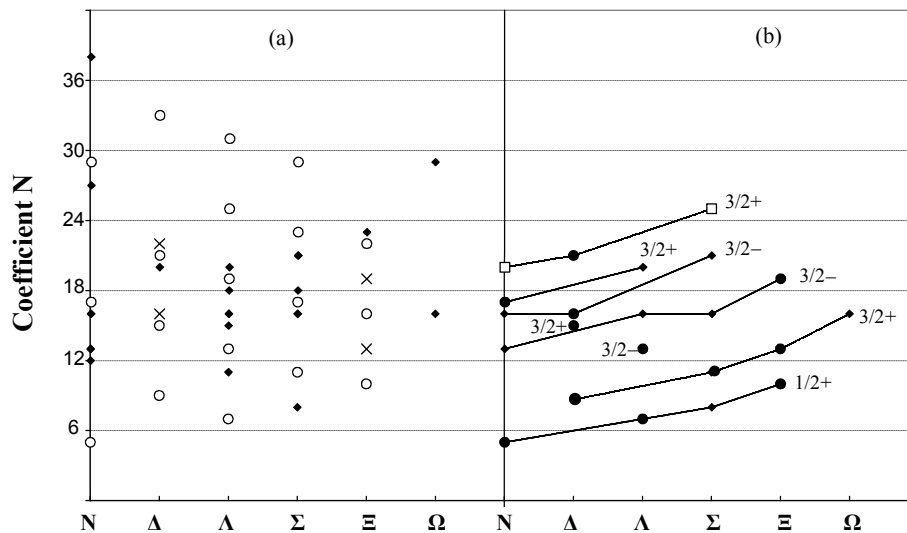


Figure 2.6 (a) Quantisation number N plotted for the six types of baryon.
 (b) The ($J^P = 3/2^-$) groups are shown relative to ($J^P = 3/2^+$) and ($J^P = 1/2^+$).

Figure 2.7b shows the higher ($J^P = 5/2^+$) group as having N values greater than the lower octet by ($\Delta N \approx 6-7$).

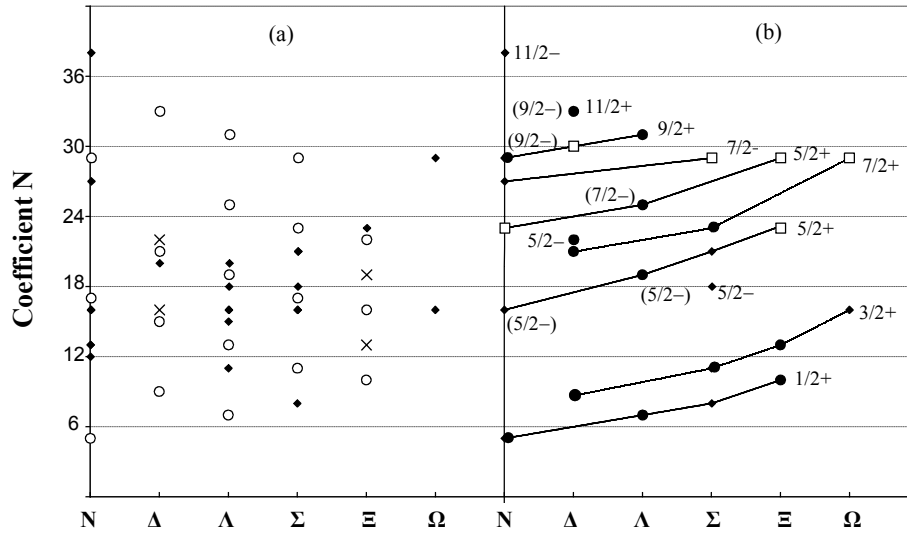


Figure 2.7 (a) Quantisation number N plotted for the six types of baryon.

(b) The higher ($J^P = 5/2^+$) group and various poorly-grouped species are shown relative to the standard ($J^P = 5/2^+$), ($J^P = 3/2^+$) and ($J^P = 1/2^+$) groups. Terms in brackets represent additional baryons with different J^P values but similar mass.

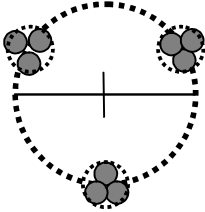
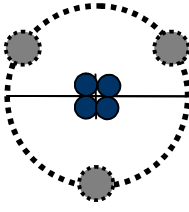
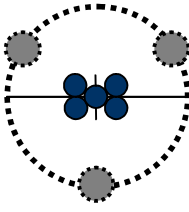
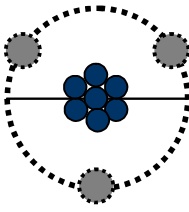
3. Strangeness

The concept of baryon strangeness is founded upon the very long lifetimes of those with the lowest mass in their group, $\Lambda(1116)$, $\Sigma(1193)$, $\Xi(1315)$, $\Omega^-(1672)$. More massive strange baryons have short lifetimes, but they conserve strangeness during rapid decay into lower baryons and mesons. Consequently, strange baryons in general must possess a certain structure which is robust and transferred during decay, until ultimately at the lowest level it survives for a relatively long time, which is governed by the lifetime discussed in Section 5.

Given the success of Eq.(2.3a) for Λ s and the patterns linking species in Figure 2.3, we will propose that the *lowest* Λ , Σ , and Ξ have something in common to account for their long lifetimes. For example, the low mass of the $\Lambda(1116)$ spin-loop, given as ($M_1 = 478\text{MeV}/c^2$) by Eq.(2.5), makes it difficult to decay into a proton with its $938\text{MeV}/c^2$ spin-loop. Higher Λ s have greater spin-loop mass and can easily decay into N or Σ . Therefore by analogy, the *long-lived* $\Sigma(1193)$, and $\Xi(1315)$, may also have low spin-loop masses of ($M_1 = 447$ and $395\text{MeV}/c^2$) for ($A = 5/6$ and $7/6$ from

Eq.(2.1)) respectively. Table 1a illustrates possible designs for these baryons, with their A and N values plus component masses. The proton has 3 trineons consisting of 3 pearls each. The others have 3 trineons of low mass ($M_1/3$), plus a central core of higher mass (M_2) comprising (N-3) components.

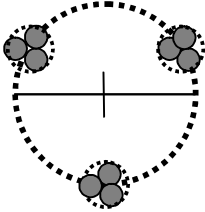
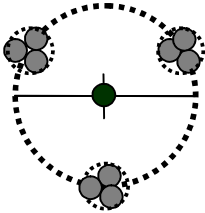
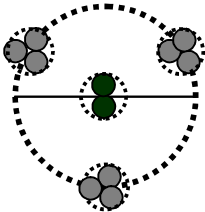
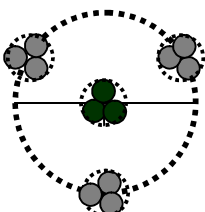
Table 1a. Proposed structure for the ($J^P = 1/2^+$) baryon octet.

| | |
|--|---|
| <p>p</p>  | <p>p(938) $1/2(1/2^+)$</p> |
| <p>Λ</p>  | <p>$\Lambda(1116)$ $0(1/2^+)$, Dy($p\pi^-, n\pi^0$) $M_1 \approx 478\text{MeV} / c^2$ $M_2 \approx 638\text{MeV} / c^2$ $A = 2/3, N = 7$</p> |
| <p>Σ</p>  | <p>$\Sigma(1190)$ $1(1/2^+)$, Dy($p\pi^0, n\pi^+, \Lambda\gamma, N\pi^-$) $M_1 \approx 446\text{MeV} / c^2$ $M_2 \approx 744\text{MeV} / c^2$ $A = 5/6, N = 8$</p> |
| <p>Ξ</p>  | <p>$\Xi(1315)$ $1/2(1/2^+)$, Dy($\Lambda\pi^0, \Lambda\pi^-$) $M_1 \approx 395\text{MeV} / c^2$ $M_2 \approx 921\text{MeV} / c^2$ $A = 7/6, N = 10$</p> |

The ($J^P = 3/2^+$) baryon decuplet reveals further how strangeness operates, although it does not appear to obey Eq.(2.3a,b) numerically. In Table 1b the $\Delta(1232)$ consists of a spin-loop only, comprising 3 trineons of 3 pearls each. A pearl here is a miniaturised *tightly bound* muonnet ($m_\mu' = (4/3)m_\mu = 140.88\text{MeV}/c^2$) as found for mesons in Paper 2. In Paper 1, a proton pearl is defined as ($m_l = m_p/9 =$

104.25MeV/c²), but the pearls in other baryons vary in mass to accommodate quantisation of action. The $\Sigma(1385)$ has a similar spin-loop but also a central core pearl which is a muonet of mass around m'_μ . The $\Xi(1530)$ has a similar spin-loop but 2 bound core pearls of mass around m'_μ each. Then $\Omega^-(1672)$ has a similar spin-loop but 3 bound core pearls of mass around m'_μ each. It is these core pearls which contribute to strangeness and can be ejected singly in the form of pions during decay. In Paper 2, the K^- consists of 4 pieces, so the decaying $\Omega^-(1672)$ generates a K^- from its core by donating one pearl from the spin-loop as it contracts into a Λ of lesser spin.

Table 1b. Proposed structure for the ($J^P = 3/2^+$) baryon decuplet.

| | |
|--|--|
| Δ  | $\Delta(1232)$ $3/2(3/2^+)$, $\Gamma = 118 \text{ MeV}$, $Dy(N\pi)$ $m = 9m'_\mu$ $\approx 1268 \left(1 - \frac{1}{37.7}\right) \text{ MeV} / c^2$ |
| Σ  | $\Sigma(1385)$ $1(3/2^+)$, $\Gamma = 36 \text{ MeV}$, $Dy(\Lambda\pi, \Sigma\pi, \Lambda\gamma)$ $m \approx 9m'_\mu + m'_\mu$ $\approx 1409 \left(1 - \frac{(2/\pi)}{37.7}\right) \text{ MeV} / c^2$ |
| Ξ  | $\Xi(1530)$ $1/2(3/2^+)$, $\Gamma = 9.1 \text{ MeV}$, $Dy(\Xi\pi)$ $m \approx 9m'_\mu + 2m'_\mu$ $\approx 1550 \left(1 - \frac{(1/2)}{37.7}\right) \text{ MeV} / c^2$ |
| Ω^-  | $\Omega^-(1672)$ $0(3/2^+)$, $\tau = 0.821 \times 10^{-10} \text{ s}$, $Dy(\Lambda K^-, \Xi\pi)$ $m \approx 9m'_\mu + 3m'_\mu$ $\approx 1691 \left(1 - \frac{(2/\pi)^2}{37.7}\right) \text{ MeV} / c^2$ |

Other groups ($J^P = 5/2^+, 7/2^+, 9/2^+$) can be based upon this octet/decuplet scheme because Figure 2.3 is linked to Figure 1, and therefore to Eqs.(2.1), (2.10a,b) and (2.11). That is, the pearl masses-squared increase to satisfy *action* requirements, rather than a linear mass law.

4. Magnetic moments of baryons.

Proton and neutron magnetic moments were calculated from a simple structural model in Paper 1. Namely, the three positively charged trineons travelled around the proton spin-loop circumference to produce $2.79\mu_N$, and one orbiting electron in the neutron produced $-4.71\mu_N$. Since other baryons are considered to be extra-complex protons, and ultimately decay into protons, their magnetic moments probably have similar structural origins as follows.

First of all, we presume that charge is distributed throughout a baryon, so that charge/mass ratio of the spin loop is the same whether or not the baryon has a core particle. Then the baryon spin-loop has a positive magnetic moment like the proton:

$$\mu_b = +(q\hbar / 2M) = +(q/e)(e\hbar / 2m_p)(m_p / M) \quad , \quad (4.1)$$

where q is the effective charge and M is the mass. Therefore, published standardised magnetic moments must be multiplied by (M/m_p) to eliminate the effect of M and reveal coefficient (q/e) , see column 3 in Table 2.

Second, for the neutral baryon, a co-rotating heavy-electron at radius r_{he} will produce a *negative* magnetic moment:

$$\mu_{he} = -(r_{he} / r_b)(e\hbar / 2M) \quad , \quad (4.2)$$

where r_b is the baryon spin radius from Eq.(2.6a) when $(M_1 \rightarrow M)$. In Table 2, C_μ is the coefficient of the magnetic moment generated by N_e such electrons, ie. ($C_\mu = -N_e(r_{he}/r_b)$). It is calculated from the difference between the new and original states, (eg. $n - p = -1.913 - 2.793 = -4.706$). This negative coefficient counteracts (q/e) of the positive spin-loop.

Heavy-electron mass m_{he} is given by:

$$\frac{m_{he}}{m_e} = \frac{r_{oe}}{r_{he}} = \frac{r_{oe}}{r_b} \times \frac{r_b}{r_{he}} \quad , \quad (4.3)$$

where $(r_{oe} = e^2/m_e c^2)$ is the classical electron radius. Ideally, heavy-electron mass should account for the difference between the bare positive baryon and its total mass; ($N_e m_{he} \approx \Delta M$), as in Σ^- and the neutron. Even if the bare baryon is not observed by

itself, (e.g., Λ^+ , Ξ^+ , Ω^+), its magnetic moment must be around (3) or (9) in C_μ , so that (m_{he}/m_e) can be estimated. This leads to an estimated mass difference. For example, between Ξ^- and Ξ^0 it is $(2 \times 9.59 - 3.95 = 15.23)m_e$, which compares roughly with the measured value $(13.4m_e)$. Exact correspondence is not expected because the heavy-electron orbit for Ξ^0 is not related to that for Ξ^- .

Table 2 Baryon magnetic moments interpreted in terms of one or two electrons orbiting a proton-type positively charged spin-loop.

| | μ_N | q/e | C_μ | N_e | r_{he}/r_b | r_{oe}/r_b | $N_e \times m_{he}/m_e$ | $\Delta M/m_e$ | $\ln(r_{he}/r_b)$ |
|-------------|---------|--------|---------------------------------|-------|--------------|--------------|-------------------------|-------------------------------|-----------------------|
| p | 2.793 | 2.793 | | | | | | | |
| n | -1.913 | -1.913 | n - p -4.706 | 1 | 4.706 | 13.4 | 2.85 | n-p 2.53 | $\pi[1/2]$ |
| Λ^0 | -0.613 | -0.729 | $\Lambda^0-(3)$ (-3.73) | 1 | (3.73) | 15.9 | (4.27) | | $\pi[\pi/e^2]$ |
| Σ^+ | 2.458 | 3.116 | | | | | | | |
| Σ^- | -1.160 | -1.480 | $\Sigma^- - \Sigma^+$ -4.596 | 2 | 2.30 | 17.0 | 2 x 7.39 | $\Sigma^- - \Sigma^+$ 15.8 | $\pi[2/e^2]$ |
| Ξ^0 | -1.250 | -1.752 | $\Xi^0-(3)$ (-4.75) | 1 | (4.75) | 18.8 | (3.95) | | $\pi[1/2]$ |
| Ξ^- | -0.651 | -0.916 | $\Xi^--(3)$ (-3.92) | 2 | (1.96) | 18.8 | (2 x 9.59) | $\Xi^- - \Xi^0$ 13.4 | $\pi[\pi/2e^2]$ |
| Ω^- | -2.02 | -3.601 | $\Omega^--(9)$ (-12.6) | 2 | (2.10) | 7.96 | (2 x 3.79) | | $\pi[(2/e^2)(e/\pi)]$ |

Notes: Column μ_N is the measured moment in nuclear magnetons; q is the effective charge in the baryon; C_μ is the coefficient of magnetic moment attributable to the number N_e of orbiting heavy-electron(s); r_{he} is the heavy-electron radius around the baryon core; (r_{oe}/r_b) is the free electron radius relative to the baryon spin-loop radius, used for calculating the heavy-electron mass ($m_{he}/m_e = r_{oe}/r_{he}$) for N_e electrons; ΔM is the *measured* increase in baryon mass being attributed to the heavy-electron(s). Values in round brackets are theoretical *estimates* for unmeasured items. For Ω^- , factor (9) in C_μ is due to its spin (3/2) which increases its spin-loop radius r_b by 3; this then affects r_{he} and m_{he} .

As was discovered for the neutron in Paper 1, the relative size of the heavy-electron radius (r_{he}/r_b) satisfies an action integral which serves to stabilise the orbit. The electron sends a feeler guidewave down to the baryon spin-loop which then reflects it back. If the *equivalent* guidewave charge is δe and its mass δm_{he} , then ($\delta e^2/c = \delta m_{he} c r_{he}$); so the guidewave action integral can be derived by differentiating $\ln(r_{he}/r_b) = \pi[x]$ to get:

$$\int_{2\pi r_b}^{2\pi r_{he}} \frac{\delta e^2}{z} dt \approx [x] \int_0^{2\pi} \frac{\delta m_{he}}{2} c r_{he} d\theta \quad , \quad (4.4)$$

where $[x]$ is a weighting coefficient given in the last column of Table 2. For Ω^- , this coefficient contains a factor (e/π) which will go over to the left side of Eq.(4.4) to signify gluon involvement, as seen previously in the proton.

The magnetic moment of Σ^+ is anomalously high like the proton and it may be expressed in a similar way, as far as data accuracy allows:

$$\begin{aligned} \mu &= (e\hbar/2M)[3.116 \pm 0.013] \quad (4.5) \\ &\approx (e\hbar/2M) \times 3 \left\{ 1 + \frac{1}{[(2\pi\alpha^{-1} + 1)]} \right\} \left\{ 1 + \left(\frac{(\pi/2)137(\pi/e_n)}{[137(2/\pi)]^2} \right) \left[1 + \left(\frac{(3)24}{24^2} \right) \right] \right\} . \end{aligned}$$

trineons pearls

As for the proton, ($\alpha \approx 137^{-1}$) is the fine structure constant, and there are 24 gluonic-loops constituting a pearl. Each of the three trineons has charge e^+ , but only unit charge emanates from the spin-loop overall. However, in contrast to the proton, these trineons are aligned *parallel* to their spin-loop and have a reduced weighting factor of $(\pi/2)$. The pearls are also *parallel*; therefore, a higher energy state for Σ^+ magnetic moment results from these parallel alignments.

In Table 2, the derivation of 2 heavy-electron masses for Σ^- produces ($N_e \times m_{he}/m_e = 2 \times 7.39$). However, the fuller derivation, which allows for guidewave binding analogous to Eq.(5.10) of Paper 2, gives ($Nm_{he}/m_e = 2 \times 7.82$) which is nearer the measured ($\Delta M/m_e$). In a similar way, for $(\Xi^- - \Xi^+)$ we could estimate ($Nm_{he}/m_e = 2 \times 7.47$), given that r_{he} evaluates to 0.2938fm.

It is appropriate here to mention the Δ^{++} , although its magnetic moment has not been measured. This baryon has the structure of a positive spin-loop orbited by a heavy-*positron*, which is held in place by its own electromagnetic guidewave force just like a heavy-electron is bound onto a proton.

5. Lifetimes of baryons

Analogous to the neutron in Paper 1, the mean lifetimes of the 4 long-lived baryons may be governed by the presence of an orbiting heavy-electron. Given the heavy-electron period ($t_{\text{he}} = 2\pi r_{\text{he}} / c$) and baryon spin-loop radius r_b from Eq.(2.6b), then:

$$t_{\text{he}} = (2Jh / Mc^2)(r_{\text{he}} / r_b) \quad . \quad (5.1)$$

Table 3 lists the (r_{he} / r_b) values from Table 2 and the calculated t_{he} values, with the measured lifetimes τ_b . Now if we say $(c\tau_b)$ is equal to a number N_b of heavy-electron circumferences (ct_{he}), then upon taking logarithms, we have for Σ^- say:

$$\ln(c\tau_b / ct_{\text{he}}) \approx 30.55 \approx 137\pi(\pi/2) / 3e_n^2 \quad . \quad (5.2)$$

By differentiating this and introducing $(e^2/c = m_{\text{he}}cr_{\text{he}})$, an expression for the electromagnetic action around the N_b circumferences may now be obtained:

$$\int_{(2\pi r_{\text{he}}(\pi/2))}^{N_b(2\pi r_{\text{he}}(\pi/2))} \frac{e^2}{z'} dt \approx 137 \times \int_0^{2\pi} \frac{m_{\text{he}}}{2} cr_{\text{he}} \left(\frac{1}{e_n^2} \right) \frac{d\theta}{3} \quad . \quad (5.3)$$

Table 3 Measured baryon lifetimes τ_b relative to the calculated heavy electron periods t_{he} . The logarithm is roughly constant, except for Ω^- . Baryon Σ^+ has been added because a similar decay law may be operating around its spin-loop.

| | r_{he}/r_b | $t_{\text{he}} (10^{-23})$ secs | $\tau_b (10^{-10})$ secs | τ_b / t_{he} (10^{13}) | $\ln(\tau_b/t_{\text{he}})$ |
|-------------|---------------------|------------------------------------|-----------------------------|---|-----------------------------|
| Λ^0 | (3.73) | 1.390 | 2.631 | 1.893 | 30.57 |
| Σ^- | 2.30 | 0.796 | 1.479 | 1.858 | 30.55 |
| Ξ^0 | (4.75) | 1.495 | 2.90 | 1.94 | 30.60 |
| Ξ^- | (1.96) | 0.617 | 1.639 | 2.65 | 30.91 |
| Ω^- | (2.10) | 1.56 | 0.822 | 0.527 | 29.29 |
| Σ^+ | (1.0) | (0.347) | 0.8018 | (2.31) | (30.77) |

The integral unit distance $(2\pi r_{\text{he}}(\pi/2))$ is the full length of the pearly helix structure around the heavy-electron, rotating at velocity $c' = c(\pi/2)$. Length $(z' = c't)$ is therefore

the instantaneous length around this helix, over N_b orbits in total. Mean distance $c\tau_b$ is thought to represent a coherence length for the guidewaves operating around the heavy-electron, which govern its stability.

Factor e_n^{-2} on the right of Eq.(5.3) represents third harmonic guidewaves for stabilising the 3 components of the heavy-electron; in agreement with the original neutron equation, Eq.(10.3.4) in Paper 1. Action for the baryons is approximately half that for the neutron. It is apparent that larger orbit periods t_{he} usually correspond with longer lifetimes. Baryon Σ^+ has been included in Table 3 for comparison, and could indicate that a similar decay law is operating around the 3 trineons of its spin-loop.

6. Conclusions.

Baryons have been described as being like extra-complex protons, in which the real spin-radius varies with mass. For many baryons, mass-squared is a function of spin, and quantised action. Empirical magnetic moments have been explained in terms of a positively charged baryon spin-loop surrounded by one or two heavy-electrons. Finally, lifetime of a baryon appears to be governed by guidewave coherence around these structures. As for the proton and mesons, mass is localised energy so the Higgs mechanism is unnecessary.

Acknowledgements

I would like to thank Imperial College Library and R. Simpson for typing.

Appendix A: Compatibility with Standard Model

The model for an isolated proton was very successful at explaining the Yukawa potential, the reality of spin and anomalous magnetic moment. On the other hand, the Standard Model of particle interactions has been very successful at accounting for data from high energy collision experiments. The conceptual differences between these models can be explained if particles in collisions generate aspects not immediately apparent in static models. That is, trineons in the proton need to behave like up, down, and strange quarks in high energy collisions. On average over many collisions, anti-quarks may even appear to be mixed with quarks in deep inelastic lepton-nucleon scattering experiments.

Consider Figure A.1 wherein the proton of Paper 1 is depicted as 3 trineons travelling around the spin-loop at the velocity of light. Each trineon has a charge (+e) but only emits an electromagnetic field due to (+e/3) into the *exterior* space, so the proton's total external charge is (+e) as observed. Trineons also emit an e.m field in the direction of travel *around* the spin-loop, equivalent to (+2e/3) each.

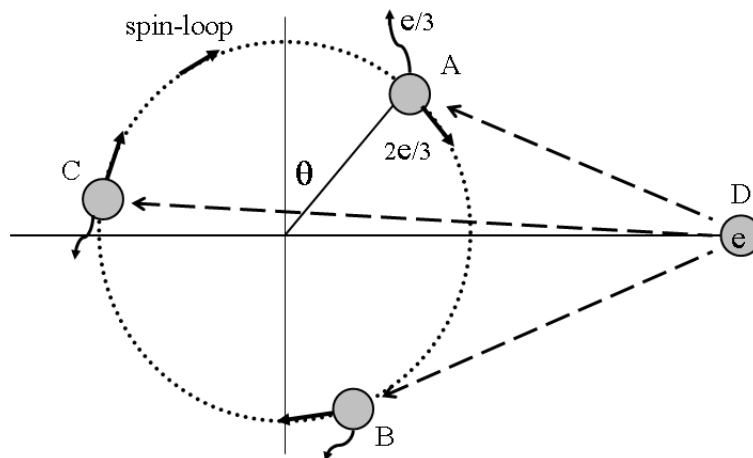


Fig.A.1 A schematic proton consisting of 3 trineons in the spin-loop with external and internal electromagnetic fields due to charge ($e/3$) and ($2e/3$), as experienced by an incident charged particle D.

Consequently, it is proposed that an energetic incident charged particle D could approach one of the trineons closely and experience an interaction which depends upon the position and *direction* of that trineon. For example, D on A will vary as $[e/3 + (2e/3)\cos(\theta)]$, whereas D on B will vary as $[e/3 + (2e/3)\cos(\theta+120^\circ)]$, and D on C will vary as $[e/3 + (2e/3)\cos(\theta+240^\circ)]$. These 3 possibilities for interaction of particle D with a proton are shown overlaid in Figure A.2. Clearly the effective *interaction charge* for a trineon can vary from ($3e/3$) to ($-e/3$).

For correspondence with the Standard Model, we require A(+ $2e/3$), B(- $e/3$), and C(+ $2e/3$), which occur at ($\theta = 60^\circ$) where the squared values are nearest to each other: A($4e^2/9$), B($e^2/9$), C($4e^2/9$). It happens that the average of $[e/3 + (2e/3)\cos(\theta)]^2$ over one spin-loop cycle is $e^2/3$, which is also the average of quark charges-squared ($4e^2/9 + 4e^2/9 + e^2/9$)/3. The A,B,C, nominations are interchangeable at ($\theta = 120^\circ$, 240°).

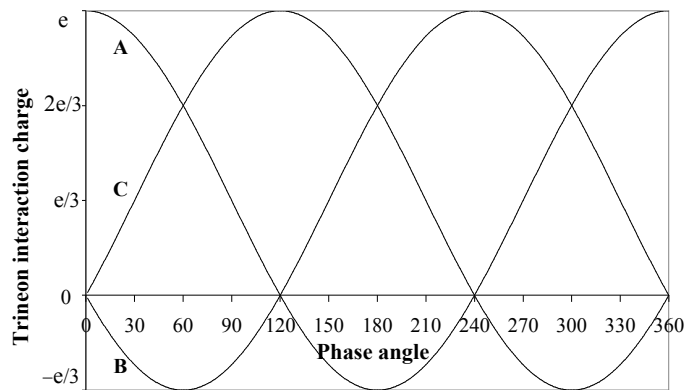


Fig.A.2 Variation of *interaction charge* for trineons A,B,C.

Thus, the appearance of a negative *interaction charge* ($-e/3$) within a positive proton is remarkable. This only happens for inelastic collision processes where a trineon reacts according to its *internal* mechanism and *direction* of travel. Trineons are tightly confined by strong force gluons within a proton, so any collision of an incident particle with a single trineon might appear to involve a quark of spin (1/2).

For the neutron model in Paper 1, a heavy-electron closely orbits the proton to neutralise its positive charge. Then if this heavy-electron joins with trineon A say, in opposing incident particle D, the effective *interaction charges* would be $A(-e/3)$, $B(-e/3)$, and $C(2e/3)$ as required. This proposed combining-process for a neutron will also be required for the neutral baryons.

References

Wayte R. (Paper 1) A model of the proton. www.vixra.org/abs/1008.0049

Wayte R. (Paper 2) A model of mesons. www.vixra.org/abs/1109.0040

Amsler C et al. (2008) Phys Lett B667, 1

Perkins D H (2000) Introduction to High Energy Physics, 4th ed, Cam Univ Press